Advances in Image And Video Processing

TABLE OF CONTENTS

EDITORIAL ADVISORY BOARD

DISCLAIMER

All the contributions are published in good faith and intentions to promote and encourage research activities around the globe. The contributions are property of their respective authors/owners and the journal is not responsible for any content that hurts someone's views or feelings etc.

Wavelet Based Finger Knuckle and Finger Vein Authentication System

[1]Sujata Kulkarni and [2]Ranjana Raut
[1]*Yeshwantrao Chavan College of Engineering, Nagpur;*
RSTM University of Nagpur (India)
[2]*Electronics Department, SGM University Nagpur, India;*
taresujata@yahoo.com; r24rd164@rediffmail.com

ABSTRACT

Biometrics is the prominent technology for accurate and safe detection of claim identity. This paper proposes a novel multimodal authentication system using finger knuckle (FK) and finger vein (FV). Finger Knuckle has unique bending and makes this a distinctive biometric identifier. The vein pattern of all fingers of human being is not same. Each finger of same person has different vein pattern. It is the hidden part which is not seen by normal eye sight hence less possible to forge. The system consists of proposed prototype finger knuckle and finger vein image capturing devices, formation of own FK and FV image database acquired from proposed devices. Here feature extraction of FK images is based on Walsh Wavelet Transform and FV image on Hybrid Wavelet Transform. Proposed multimodal biometric authentications integrate transformed domain features vector of FK and FV at score level fusion using Bayesian and weighted sum method. The fusion of these two modalities using Bayesian method demonstrated the recognition accuracy of 98.3% and weighted sum 98.5 %. Various weights of finger knuckle and finger vein affects the recognition accuracy. The better recognition accuracy is obtained at weight of 0.8 and 0.2. The performance index is improved i.e 98.5% and the Error equal rate is 1.5% as compare to unimodal biometric. Error equal rate is reduced by 10% than individual biometric system. For N user with M1 and M2 as test and training samples, for verification of one user, matching complexity is O (M1M2) and for N user O(M1 M2 x N). For identification, (N x M1) test samples and (N x M2) training samples are considered. So matching complexity is O [N (N-1) x M1] for each biometric. Using conventional matching the complexity is O [N (N-1) x M1 M2]. For multimodal biometric using FK and FV, matching complexity is O 2[N (N-1) x M1]. It shows great reduction in matching complexity using the proposed algorithms.

Keywords: Finger knuckle, Finger vein, Wavelet, Hybrid Wavelet, Authentication, Fusion, Error Equal Rate, ROC curve

1 Introduction

Traditional authentication systems based on password, access card, lock and key etc. have a lot of issues of stolen the card, misuse of card, forgotten password and different password attacks. Today's wireless world, transaction through internet is demanding from the users hence needs to develop an authentication system that gives more security of individual identity. Modern authentication system based on human physiological and behavioural detail gives security to personal information and not easy to forge is known as biometric recognition system. It is generally accepted that physical traits like iris, fingerprints, finger knuckle, finger vein, DNA finger print [1] can uniquely defined each member

of large population which makes them suitable for large scale identification. Reason of attraction of such traits is social acceptance and easy to use. Finger knuckle (FK) is user centric, contactless and unrestricted access control. Texture and statistical features are available and easily extracted. It is independent to any behavioural aspect. No stigma of potential criminal investigation is associated with this approach [2]. Finger vein are internal part hence impossible to forge, unique, reliable ,secure because not traceable by eye, less failure to enroll rate (FET), no issues of wet, dry, dirt like finger print. Proposed paper uses finger knuckle and finger vein as two biometrics for authentication. Unimodal biometric authentication is performed by identifying only single trait. Each biometrics system is not able to enroll all types of data. Failure to enroll is big issue in unimodal biometrics. Unimodal biometrics trait experiences a lot of problems such as noise data, spoof attacks, intra-class variation and unacceptable error rate. The advanced biometric concept known as multimodal biometric systems are used to overcomes the limitations of unimodel biometric systems. It integrates multiple evidences such as multiple units, multiple samples, and multiple traits from multiple sources of information [3]. Multimodal system can combine correlated as well uncorrelated biometric traits. Multimodal biometric is more reliable and secure due to use of multiple evidences. The integration of multiple evidences is possible using fusion techniques at different level [4]. Categories of multimodal biometric depend upon the integration of different basic units. Such system requires longer verification time thereby causing inconvenience to the users. Due to these limitations, the number of identifiers (modalities) in a multimodal biometric system is usually restricted to two or three.

The paper is organized as follows. Section 2 presents proposed multimodal system, Section 3 presents finger knuckle and FK database Section 4 describe finger vein acquisition devices and FV data base, Section 5 discuss feature vector generation using Kekre and Hybrid wavelet transform. Section 6 discusses fusion of two modalities. Results and conclusion are presented in Section 7.

2 Proposed Multimodal Authentication System

The Proposed system uses finger knuckle and finger vein as biometric traits and integrate transformed domain features extracted from them at matching score level. It mainly consists of three components: finger knuckle unit, finger vein unit and score level fusion unit. Finger knuckle recognition is responsible for matching the input finger knuckle against the finger knuckle templates stored in the database to obtain finger knuckle matching scores. Finger vein recognition is responsible for matching the input finger vein against the finger vein templates to obtain finger vein matching score. This score is normalized using Min-max normalization. Score level fusion is obtained using weighted sum and Bayesian rule. It integrates matching scores from finger knuckle and finger vein recognition block and forms the new scores which make the final decision. The framework of proposed multimodal biometric authentication system shows the integration of finger knuckle and finger vein at score level as shown in Figure1
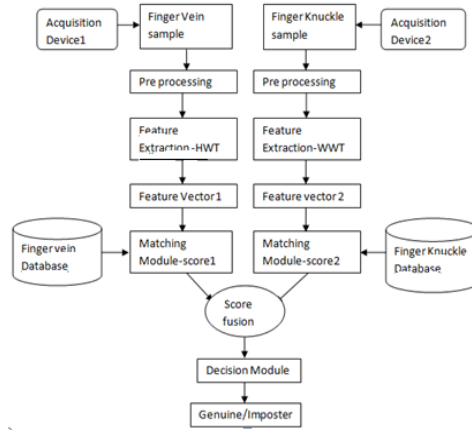
Figure 1: Framework of Proposed Multimodal System

3 Proposed Finger Knuckle Acquisition Device

Proposed prototype Finger knuckle capturing device is composed of light weight acrylic box with white background, finger supporter and digital camera (SonyDSC-W380) as shown in Figure 2. Camera captures the FK images with white and black background. The captured images with black background are darker than white background. Hence images with white background are used for reorganization.

(a)   (b)   (c)
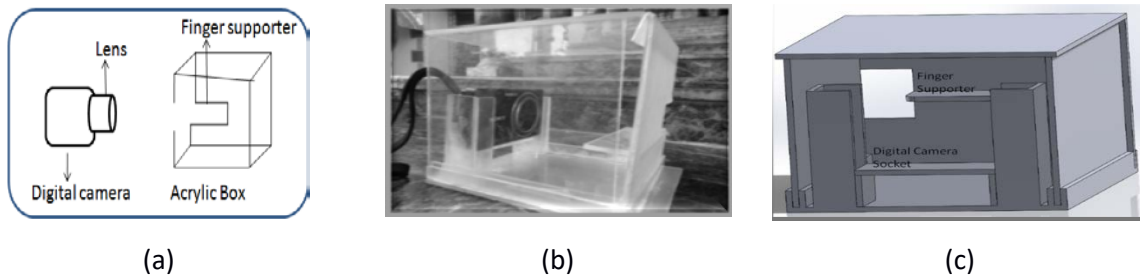
Figure 2: Finger knuckle acquisition device (a) prototype device (b) frame work of device (c) Modified FKP device [20]

During acquisition, user places finger from the notch at front side of device on finger supporter. Notch size is optimum, so user with any finger size can place finger on supporter and FK images can be acquired. During   FK images acquisition, translation or rotations of finger take place. Such movement can increase the variation in finger knuckle feature of authenticate user. To overcome these limitations, device uses folding bar as guiding structure for finger tips and part of back side of finger. Finger bracket is designed for this purpose. The modification in capturing device is made with proper design using Solid Works 2013.

- In modified device, finger notch is flexible and mounted on the finger supporter.
- Modified FKP device is compact in size (140 mm x 130 mm x 90 mm), cost effective, user friendly and acquire FK images with high resolution (4300 x 3200 pixels).
- Distance between the camera and knuckle is 89 mm and with white back ground.
- The distance between the camera and supporter is 89.04 mm
- Height of the device is reduced to 90 mm to avoid outside reflection during acquisition of FK images.

The proposed proto type finger knuckle acquisition device survives under uncontrolled lighting conditions and deformation due to finger orientation and perspective projection. Hence, users of the biometric authentication system can be relieved from the careful planning of acquisition environment

and unnatural hand orientation during capture. The FK images used in proposed system are acquired by ordinary cameras equipped on portable devices.

3.1   Finger knuckle image database

As per hand geometry, number of finger is available for acquisition. Proposed system indented to capture only the middle knuckle of right index and right middle finger. Among five fingers, lower, middle and upper knuckles are present only on the four fingers except thumb. Small finger knuckle is too small in area. Database consists of finger knuckle of right index and middle knuckle of all classes to cover the entire population. FK image database consists of 50 users (18 to 68 years) from an educational institute including different categories such as VIP, teaching, non-teaching, students and workers. To consider variant finger knuckle location and orientation, FK images are acquired in two phases with average interval of days and time. By using proposed image acquisition devices, Images from the same finger collected at different time are similar to each other while images from different fingers are different; this implies that FKP has potential for personal identification.   Figure 3 shows some of sample FK images acquired from the proposed device.

User1_1index...	User1_5index	User1_1 middle...	User1_5middle
User1_1index..	User1_5index	User1_1 middle...	User1_5middle
User1_1index…	User1_5index	User1_1 middle...	User1_5middle
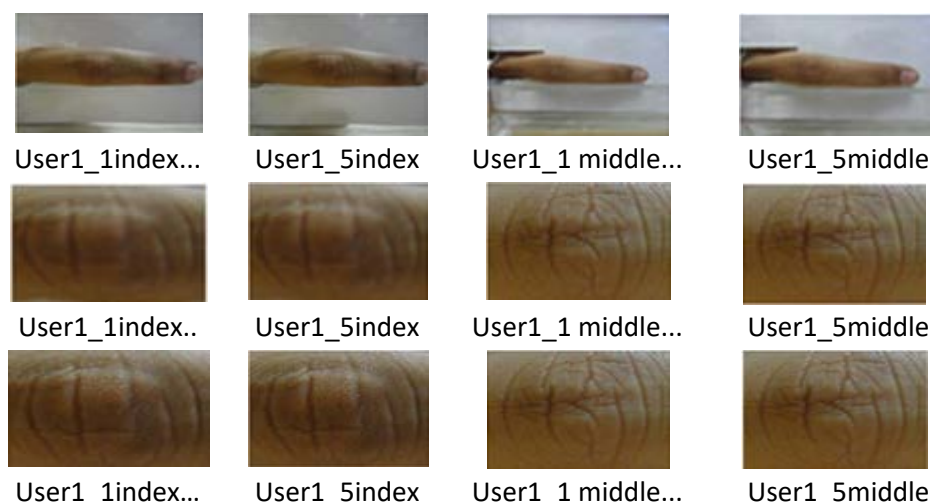
Figure 3: Some of sample finger Knuckle images acquired from proposed prototype acquisition device(a)Raw FK (b) Cropped FK (c) Resized FK samples [20]

4 Proposed Finger Vein acquisition Device

Proposed FV image acquisition device consists of LEDs assembly, capturing unit, power supply unit, and display. Finger vein acquisition device is based on NIR optical source and simple IR camera to capture the vein pattern. NIR assembly consists of series alignment of NIR LEDs of 750 nm non-contact with finger as shown in figure 4. Numbers of LEDs are chosen to cover whole finger of any person as thickness of finger changes person to person such as fat, medium and thin finger. Finger is placed on NIR assembly. When power in ON, light is radiated   from the NIR LEDs passes through the finger and is absorbed by haemoglobin of blood and shows dark blood vessel pattern. This pattern is captured by IR camera. Simple webcam without IR filter act as IR camera. NIR imaging is safe because it penetrate only the superficial area of the finger. When light is radiated in the finger, temperature of the skin increases, but it is controlled by adjusting operational parameter of LED that make LED within safe temperature range [10]. In this system, finger is in non-contact with NIR LEDs and acquisition of vein is in milliseconds hence safer. Here IR camera is installed on laptop. Driver of laptop are changed because webcam is inbuilt in laptop which senses the visible light while IR camera senses the IR light.

If the display screen is desktop, then driver are not changed. The physical set up finger vein acquisition is as shown in figure 5
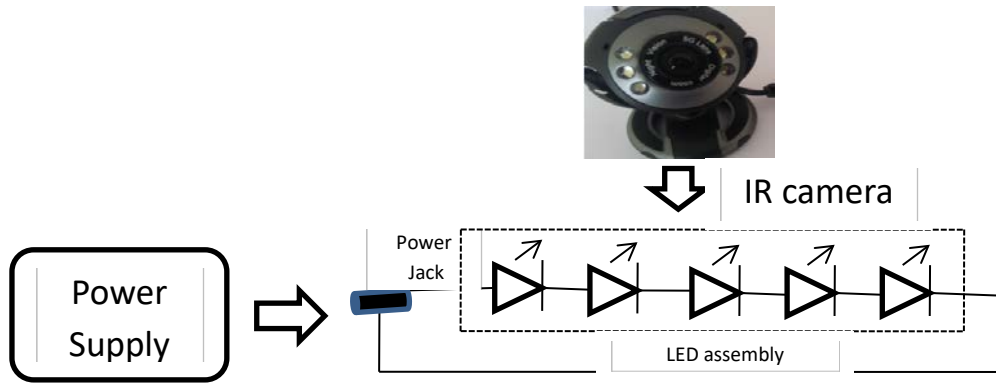

IR camera

Power Jack

Power Supply

LED assembly

Figure 4: Optical source and camera set up of Finger vein device [21]

Power supply

Potentiometer

IR Camera

Finger Supporter

NIR Light Source

USB Interface

Finger window(25cmx25cm)

(a)

(b)

(c)
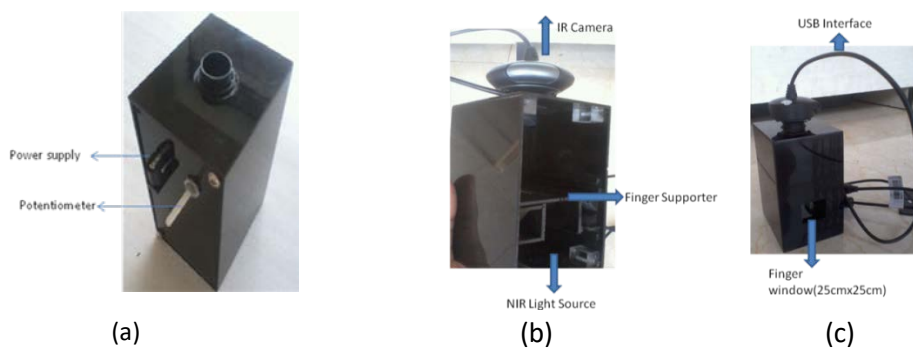
Figure 5: Physical set up of Finger Vein Device (a) Back view (b) Internal framework (c) Font view [21]

4.1 Finger Vein Image database

Total 50 users are considered during enrolment procedure. Ten samples of each unit are taken so total 20 samples of each user. Database of 50 users is formed using 500 finger vein samples at different orientation. Database covers different categories like VIP person to worker class users and senior citizen. It is further classified as gender and age. Users of age of 18 to 65, fatty, weak and moderate health persons are involved. Finger vein samples of users with different categories are taken in order to analyze the failure to enrolled rate. It is noted that, three user could not enroll finger vein samples due to weakness whose haemoglobin level is not up to the mark. Another two users are not able to enroll due to their natural finger style. Alignment of vein pattern is not proper because of natural bend at first knuckle. Sample finger vein image are as shown in figure 6. The captured raw finger vein samples are of size 640 x 480 as shown in figure 6 (a) and (b). From the original vein samples middle part of fingers vein are cropped to obtain region of interest with finger geometry.

User1_RI_1...   User1_RI_10   User1_RM_1 ...   User1_RM_10

User60_RI_1...   User60_RI_10   User60_RM_1...User60_RM_10

(a)

(b)
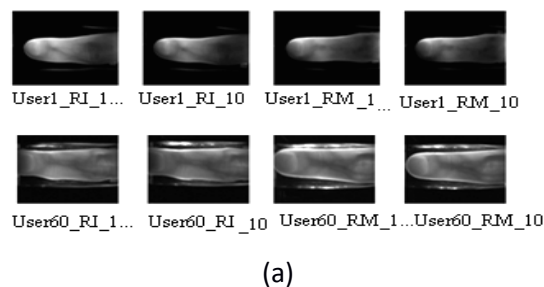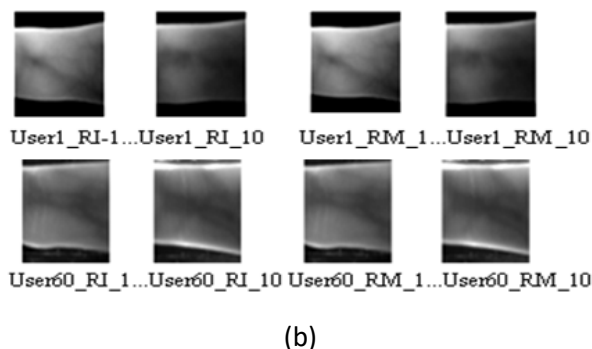
Figure 6: Acquired Finger vein pattern (a) Raw finger vein pattern (b) cropped Finger vein samples
Finger knuckle and Finger vein Enhancement

Images captured from the modified FK device are raw images. These images are enhanced to get better clarity of unique features such as ridges, creases around the phalangeal joint of finger knuckle surface. This is very important step to improve the recognition. We use Weiner filter and reflection removal as pre-processing step to enhance the quality of FK images. Images with many edges are handled by local wiener filter. Hence de noising all the FKP is done using Winner filter [17] .Original images has curvature surface hence results in non-uniform reflection. To obtain well distributed texture, we use the reflection removal technique [15]. The reflection filtered image is enhanced image from which feature are extracted. Features are extraction using Kekre Wavelet Transform. During the enrolment stage, the raw vein pattern shows noise due to high temperature and transmission noise created by the IR radiation. Actual features of vein pattern get hide due to such noise. Hence need to apply the pre-processing method to get better clarity from the raw samples.

This paper explores the bilateral and median filtering techniques for noise removal. Median filter is used to remove noise in the form of defective pixel and make the samples noise free. Edge preservation is another property of median filter which is the important information for vein samples [19]. But edge retention using median is not applicable for all condition hence second de noising bilateral technique is used. Contrast adaptive histogram reduces amplified noise by clipping the histogram. Histogram is clipped at specific value called as clip limit. Generally amplification can be limited by common value between 3 and 4.The amplified part beyond the clip limit is uniformly redistributed among all histogram [11, 15] and get enhanced vein pattern.

5 Feature Vector Extraction of Finger Knuckle

Walsh is an orthogonal transform, so Walsh Wavelet is generated from Walsh transform [118]. 16 x 16 Walsh Wavelet from 4 x 4 Walsh transform matrix as shown in Figure 7.
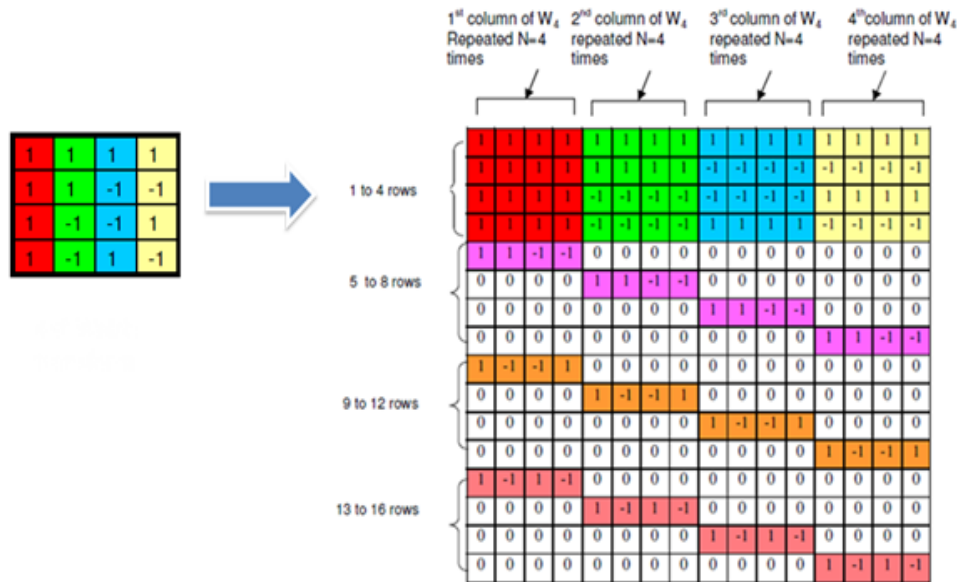
Figure 7: Walsh wavelet transform

The ROI is selected to be of size 128 x 256. The Walsh wavelet transform of size 128 x 128 is selected. Extract all the features of knuckle from the flow shown in figure 8. These features are the energy coefficient calculated by following equation 1.
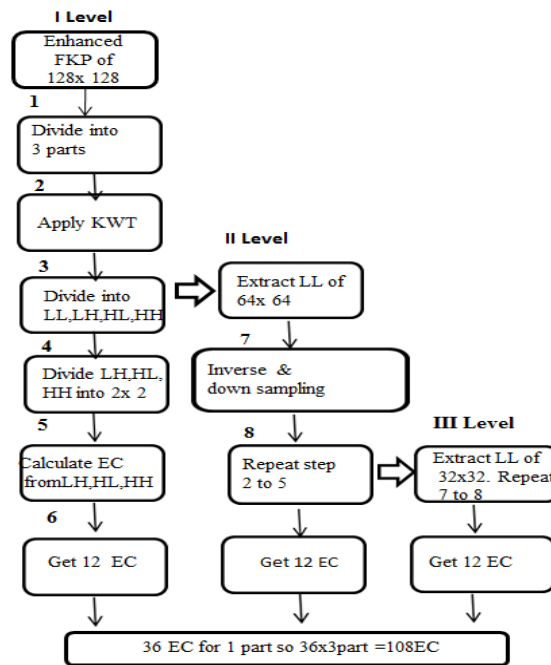
Figure 8: Flow of Feature extraction using WWT

$$WE_{LC} = \sum_{i=0}^{w-1} \sum_{j=0}^{w-1} WC(i,j)^2 \qquad (1)$$

Where L=0, 1, 2; C = 0(LH), 1(HL), 2(HH) and W is the size of wavelet component in the different level i.e. 64, 32, 16 respectively. Similarly a set of 4 wavelet coefficients are obtained from HL and HH. The values of these 3 set of coefficients give 12 features from the first level, 12 from second and 12 from third so total 36 energy coefficients for left part of enhanced sample. The same procedure is carried out on right and centre block .Hence, the final feature vector has 108 feature values. The values of the feature vector are taken without normalization. Such feature vectors are generated for training 7

samples of each user and over database of 50 users. Therefore, the training samples are 350. A matrix file of all the feature vector of 350 samples is created.

5.1   Feature Vector Extraction of Finger Vein

Hybrid Wavelet Transform is used for combining the traits of two different orthogonal transform wavelets to exploit the strengths of both transform wavelets. The hybrid wavelet transform matrix of size N x N (say 'TAB') can be generated from two orthogonal transform matrices (say A and B respectively) with sizes p x p and q x q. where N = p*q = pq. Hybrid transform matrix is generated from matrix A and B. Proposed finger vein recognition system developed the hybrid wavelet using Kekre and DCT for global feature extraction as represented in figure 9.

$$A=\begin{bmatrix} a_{11} & a_{12} & \cdots & a_{1p} \\ a_{21} & a_{22} & \cdots & a_{2p} \\ \vdots & \vdots & \cdots & \vdots \\ a_{p1} & a_{p2} & \cdots & a_{pp} \end{bmatrix} \qquad B=\begin{bmatrix} b_{11} & b_{12} & \cdots & b_{1q} \\ b_{21} & b_{22} & \cdots & b_{2q} \\ \vdots & \vdots & \cdots & \vdots \\ b_{q1} & b_{q2} & \cdots & b_{qq} \end{bmatrix}$$
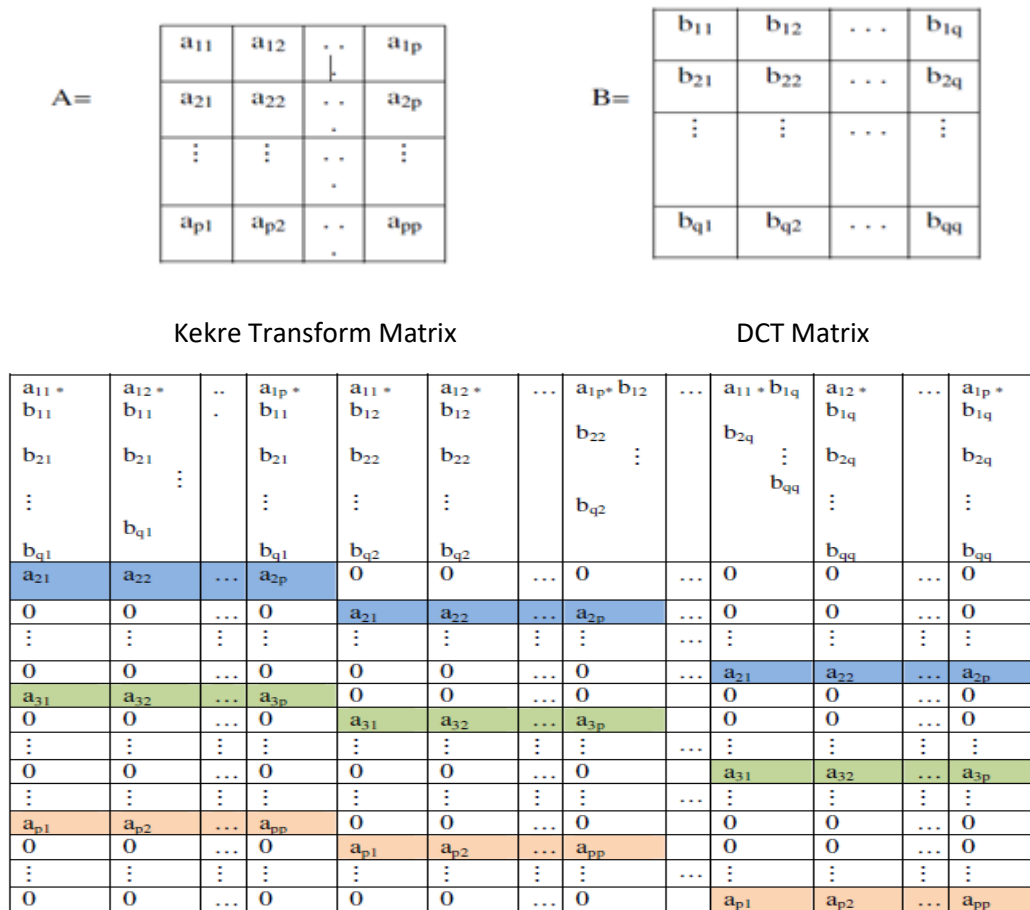
Kekre Transform Matrix   DCT Matrix

$a_{11} \cdot b_{11}$, b_{21}, ⋮, b_{q1}	$a_{12} \cdot b_{11}$, b_{21}, ⋮, b_{q1}	..	$a_{1p} \cdot b_{11}$, b_{21}, ⋮, b_{q1}	$a_{11} \cdot b_{12}$, b_{22}, ⋮, b_{q2}	$a_{12} \cdot b_{12}$, b_{22}, ⋮, b_{q2}	...	$a_{1p} \cdot b_{12}$, b_{22}, ⋮, b_{q2}	...	$a_{11} \cdot b_{1q}$, b_{2q}, b_{qq}	$a_{12} \cdot b_{1q}$, b_{2q}, ⋮, b_{qq}	...	$a_{1p} \cdot b_{1q}$, b_{2q}, ⋮, b_{qq}
a_{21}	a_{22}	...	a_{2p}	0	0	...	0	...	0	0	...	0
0	0	...	0	a_{21}	a_{22}	...	a_{2p}	...	0	0	...	0
⋮	⋮	⋮	⋮	⋮	⋮	⋮	⋮	...	⋮	⋮	⋮	⋮
0	0	...	0	0	0	...	0	...	a_{21}	a_{22}	...	a_{2p}
a_{31}	a_{32}	...	a_{3p}	0	0	...	0		0	0	...	0
0	0	...	0	a_{31}	a_{32}	...	a_{3p}		0	0	...	0
⋮	⋮	⋮	⋮	⋮	⋮	⋮	⋮	...	⋮	⋮	⋮	⋮
0	0	...	0	0	0	...	0	...	a_{31}	a_{32}	...	a_{3p}
⋮	⋮	⋮	⋮	⋮	⋮	⋮	⋮	...	⋮	⋮	⋮	⋮
a_{p1}	a_{p2}	...	a_{pp}	0	0	...	0		0	0	...	0
0	0	...	0	a_{p1}	a_{p2}	...	a_{pp}		0	0	...	0
⋮	⋮	⋮	⋮	⋮	⋮	⋮	⋮	...	⋮	⋮	⋮	⋮
0	0	...	0	0	0	...	0		a_{p1}	a_{p2}	...	a_{pp}

**Figure 9: Hybrid Wavelet Transform from Kekre and DCT**

Here, wavelet energy feature (WEF) is used to describe the vein texture. Hybrid Wavelet (HW) Transform of the selected vein pattern ROI is taken. The wavelets will capture localized spectral information from the ROI. Use only ROI of size 128 X 128 pixels. At each level, Mth order Hybrid Wavelet matrix (M X M Size) is generated by M/4 (64X64) order Kekre Transform Matrix [24.Figure 10 shows 1st level decomposition using Hybrid Wavelets. Take 128 X 128 finger vein Image and the first level The next level of decomposition is on matrix of size N/2 X N/2 (half of the previous). This will continue K times for K level decomposition. In case of Hybrid wavelets there is a problem, as the LL components has size less than N/2 (or M in case of MP X MP size wavelet). Next level decomposition becomes difficult as at every level the size is reduced by 1/P-1 factor, as well as the down sampling is also difficult.

The proposed a novel method to overcome this issue discussed as follows. Instead of taking the LL component form the Hybrid Wavelet; take low Frequency component generated by other wavelets like Kekre Wavelet. As these wavelets have N/2 size component and generate separate set of Hybrid wavelet for each decomposition level shown in Table 1

Table 1: Wavelet Coefficients blocks for Wavelet Energy Features

Level (Image Size 128*128)	Kekre Wavelet LL Component Size	Hybrid Wavelet LL Component Size	Parameters used for WEF Generation using Hybrid Wavelets (M.P)
K=1	NA	32*32	M=32, P=4
K=2	64*64	16*16	M=16, P=4
K=3	32*32	8*8	M=8, P=4
K=4	16*16	4*4	M=4, P=4

Now, to generate the multi resolution analysis of the given Image data, here consider initial vein sample size as 128X128 Pixels.
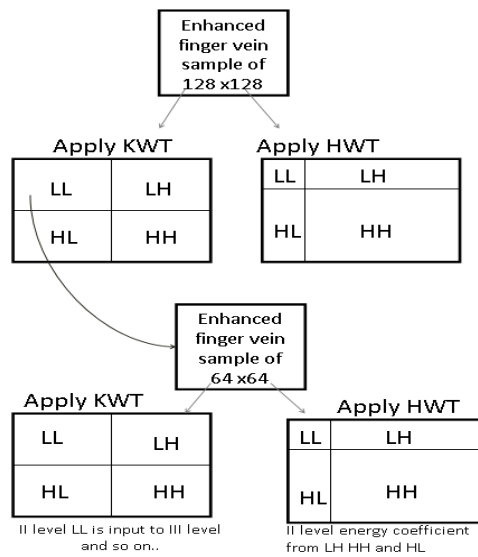
Figure 10: Transformed finger vein pattern using KWT and HWT
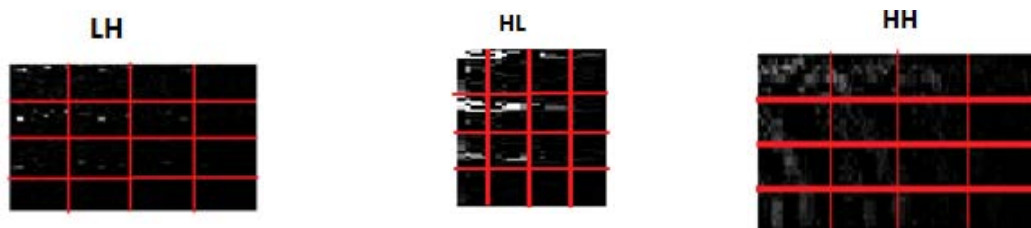
Figure 11: Energy coefficients from the Hybrid wavelet sample

$$E_i^h = \sum_{x=1}^{M} 1 \sum_{y=1}^{N} (H_i(x,y))^2 \tag{2}$$

$$E_i^v = \sum_{x=1}^{M} 1 \sum_{y=1}^{N} (V_i(x,y))^2 \tag{3}$$

$$E_i^d = \sum_{x=1}^{M} 1 \sum_{y=1}^{N} (D_i(x,y))^2 \tag{4}$$

1. Take Original Image and evaluate first level decomposition using Kekres Wavelets and Hybrid Wavelets. Use LH, HL, & HH Components of Hybrid Wavelets for generation of Wavelet Energy Distribution as per equations

2. Use LL component of Kekre Wavelet and generate next level input using Inverse Wavelet & down sampling. This will be used as input for K=2.

3. Using the input generated from Kekre Wavelet, perform Hybrid Wavelet Decomposition. For this level (K=2) the size of input image component is 64 x 64. Generate the Hybrid Wavelet by M=16 & P=4 and form the feature vector as discussed above.

4. Repeat Steps 3 & 4 for next levels and use parameters as calculated in Table 4.6 as per the procedure discussed. This procedure is shown for two levels K=1 & K=2.

Using the above mentioned procedure the feature vector is generated, the feature vector has total 144 coefficients for K=3(16 X 3X 3 = 144, 16 Coefficient Per Components X 3 Component Per Level X 3 Levels of Components). Every decomposition level has reduced component size, hence the overall wavelet component energy goes on reducing and the value of feature vector coefficients goes on diminishing. Hence, the Feature Vector is normalized Each Level wise. Figure 6 shows the feature vector normalized level wise, here we can see the energy distribution. Three sections can be seen for five decomposition levels (K=3). This feature vector is used for matching of the vein pattern. These feature vector is matching with the enroll samples of finger knuckle and finger vein is matched with Euclidean distance to generate a score.

6 Score Level Fusion using Bayesian Method

Let w_1, w_2 …. w_n represents N   users enrolled in the database. Let **x** be   the feature vector corresponding to the primary biometric. Without loss of generality, let us assume that output of the primary biometric system is of the form

$$P(\mathbf{w_i}|x), i = 1, 2, \cdots, n \tag{5}$$

where $P(W_i|\mathbf{x})$ is the probability that the test user is $W_i|_{given}$ the feature vector X. If the output of the primary biometric system is a matching score, it is converted into posterior probability using an appropriate transformation.

For the secondary biometric system, we can consider $P(W_i|\mathbf{x})$ as the prior probability of the test user being user ω_i.

Let $\mathbf{y} = [y_1, y_2, ..., y_k, y_{k+1}, y_{k+2}, ... y_m]$ be the second biometric feature vector, where y_1 through y_k are continuous variables and y_{k+1} through y_m are discrete variables. The final matching probability of user w_i, given the primary biometric feature vector X and the second biometric feature vector Y, i.e., P (w_i| x, y) is calculated using the Bayesian rule as [22]

$$P(w_i|x, y) = \frac{p(y|W_i)P(w_i|x)}{\sum_{i=1}^{n} p(y|W_i)P(w_i|x)} \tag{6}$$

Where X = input image feature vector

P (w_i|x))= Euclidean distance in terms of probability (Primary finger knuckle biometric)

P (y|w_i)) = Euclidean distance in terms of probability (Secondary finger vein biometric)

Theses Euclidean distances are converted in probability form in order to fuse at score level in the range of 0 to 1

P (w$_i$|x)) is the probability (FK) of user given the primary biometric,

P (y|w$_i$)) Where y is the probability (FV) of user given the identity claimed by the user . The scores of both primary and secondary biometric are normalized by Min-max normalization. Post score normalization, normalized average score is calculated and considered as the new score for multimodal identification system. If the correlation of claim user is less than new score, it is accepted else it is rejected from the decision module

Given a set of matching distance of finger knuckle recognition are **{d$_{fk}$}**, for k =1, 2, 3…, n, the normalization scores are given by,

$$S_{fk} = \frac{d_{fk} - min}{max - min} \tag{7}$$

Where **d$_{fk}$, S$_{fk}$** are matching distances and matching score after normalization of finger knuckle respectively. Similarly **dfv$_v$, S$_{fv}$** are the matching distances and matching score after normalization of finger vein biometric calculated using following equation as [feig].

$$S_{fv} = \frac{d_{fv} - min}{max - min} \tag{8}$$

The fusion method is tested on own finger knuckle and finger vein database consisting of 500 samples each with 10 samples of each user and each trait. So in total 1000 finger knuckles and finger veins are considered. The experimental test has shown the great improvement in the recognition accuracy of multimodal over individual biometric system which is represented in terms of TAR vs. TRR and threshold   graph as shown in Figure12.
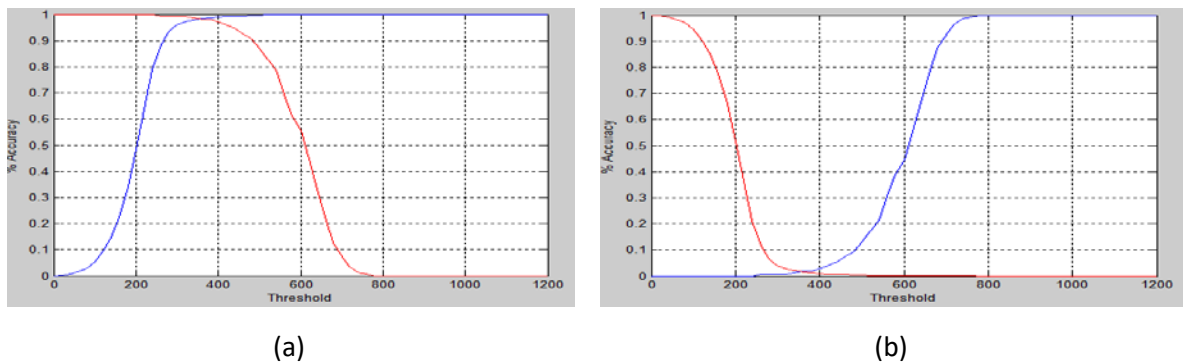

(a)   (b)

Figure 12: Recognition accuracy using Bayesian method

The graphical representation shows that the true acceptance rate increases using Bayesian fusion method. So indirectly the Error equal rate (EER) reduces as compared to the individual finger knuckle and finger vein. Table 2 shows the recognition accuracy of finger knuckle and finger vein using Bayesian method.

Table 2: Recognition Accuracy of Multimodal system using Bayesian method

Biometric	Fusion Recognition Rate (%)	
	TAR	FAR
Finger knuckle (WWT)	88.67	11.33
Finger Vein(HWT)	88.22	11.88
Score Fusion	98.3	1.7

6.1 Score Level Fusion using Weighted Sum Method

Matching algorithms for finger knuckle and finger vein based recognition system are different. In both the cases, Euclidean distances are used for matching results of finger knuckle and finger vein recognition. Therefore, matching results scores of finger vein recognition are normalized. The Min-max normalization [6] simplest technique is used. The matching score obtained from Hybrid Wavelet Transform and Walsh Wavelet Transform are fused at score level. The fusion is done using weighted sum technique.

Let Wfk and W_{fv} are weights of finger knuckle (WWT) and finger vein (HWT) respectively. The weights are given by

$$W_{fk} = \frac{c_{fk}}{c_{fk}+c_{fv}} \tag{9}$$

$$W_{fv} = \frac{c_{fv}}{c_{v}+c_{fk}} \tag{10}$$

Where C_{fk} = (TAR / total images) * 100; for Walsh wavelet transform

C_{fv} = (TAR / total images)*100;   for Hybrid wavelet transform

M_{fk} and M_{fv} are matching score of finger knuckle (WWT) and finger vein (HWT) respectively. The final score obtained after fusion [22]is as follows

$$S = W_{fk}M_{fk} + W_{fv}M_{fv} \tag{11}$$

Here Wfk and W_{fv} are their weights is the fusion score. The weights Wfk and W_{fv} are varied over the range [0, 1], such that the constraint Wfk + W_{fv} + =1 is satisfied [22].

Table 3 presents the recognition accuracy of fusion at different weights of finger knuckle and finger vein. Here, weight for finger knuckle is the range (0.9 - 0.5) and finger vein in the range (0.1 -0.5) are changed such that constraint Wfk + W_{fv} =1 is satisfied.

Table 3 presents the recognition accuracy of fusion at different weights of finger knuckle and finger vein. Here, weight for finger knuckle is the range (0.9 - 0.5) and finger vein in the range (0.1 -0.5) are changed such that constraint + =1 is satisfied.

It is observed that for recognition accuracy using multimodal recognition system is in the range of 96.5 % to 97.5% depending on the weight used for finger knuckle and finger vein traits. For finger knuckle weight in the range of 0.7 to 0.8, system has maximum recognition accuracy of 98.3 % to 98.5 %. For equal weight, recognition accuracy is 97.5 %. The recognition accuracy of unimodal system using finger knuckle and finger vein by using different algorithms is in the range of 90 %. The recognition accuracy

of unimodal system using finger knuckle and finger vein by using different algorithms is in the range of 90 to 93 %.

Table 3 Recognition Accuracy of Multimodal system using Bayesian method at different weights

W_{fk}	W_{fv}	Fusion Recognition Rate (%)
0.9	0.1	96.5
0.8	0.2	98.5
0.7	0.3	98.3
0.6	0.4	97.3
0.5	0.5	97.5

Figure 13 shows the performance of multi modal recognition system in terms of TAR Vs TRR using the weighted sum rule. Table 4 presents the recognition accuracy of multimodal system using score fusion level


(a)   (b)
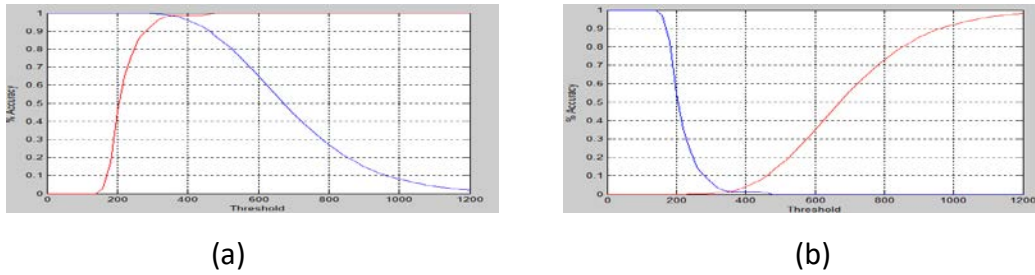
Figure 13: Recognition accuracy of multimodal biometric system using weighted sum

Table 4. Comparison of Recognition accuracy of multimodal system

Multimodal Biometric	Fusion Recognition Rate performance (%)	
	TAR	FAR
Weighted Sum	98.5	1.5
Bayesian	98.3	1.7

The ROC plot is a graphical representation of Genuine Acceptance Rate (GAR) and False Acceptance Rate (FAR). Matching decision depends upon the threshold value that shows similar or correlates the claim template to stored template. ROC curve of figure 14 shows the comparison of score fusion
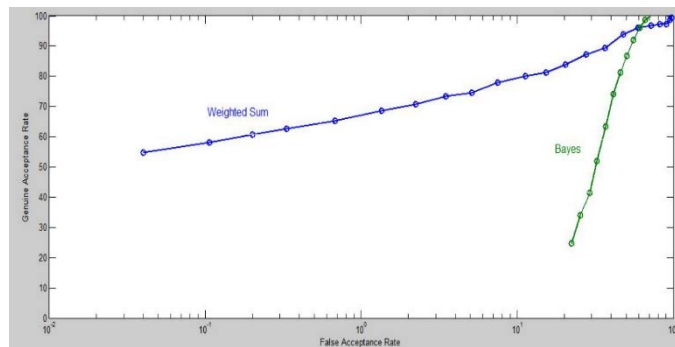
Figure 14: ROC Curve for score fusion

ROC curve shows the better performance in recognition of genuine user using weighted fusion compared to Bayesians fusion. Score level fusion using weighted sum and Bayesian achieved less False Acceptance of imposters compared to individual finger knuckle or finger vein.

The complexity of the proposed algorithm is summarized a under. Let N represent total number of user and each user has M samples. Let M1 and M2 represents number of test and training samples used such that M1+ M2 = M. So we select (M1 x N) test samples and (M2 x N) samples. For verification, each test sample Ti (Ti for i = 1 to 3) is compared with all training samples Trj (Trj for j =1 to 7), So for one user matching complexity is O(M1M2) and for N user O(M1M2 x N).

For identification, (N xM1) test samples and (NX M2) training samples are considered. So matching complexity is O [N (N-1) x M1] for each biometric. Using conventional matching the complexity is O [N (N-1) X M1 M2]. For multimodal biometric using FK and FV, matching complexity is O 2[N (N-1) x M1]. For N = 50 users and M1 = 3 (test samples) and M2 = 7(training samples), complexity using conventional method is 51450 tests need to perform. Proposed algorithms performed 7350 tests for matching, which shows great improvement in time complexity. However the complexities of algorithms depend on number of features used to represents the samples in the database. If each sample is represented by P features, then the complexity of the algorithm is O [P x N (N-1) x M1]. In the proposed multimodal recognition algorithm, 500 finger knuckle and 500 finger vein samples are used . For fusion at score level using weighted sum, requires 500 additions and 1000 multiplications. In general, number of additions and multiplication required would be N and 2N.

7 Results and Conclusion

Proposed multimodal biometric authentication integrates transformed finger knuckle and finger vein features using score level fusion. To demonstrate the efficiency recognition, experiments based on own finger knuckle and finger vein database performed. The finger knuckle and finger vein features are successfully integrated using Bayesian and weighted sum method. The recognition accuracy of integrated biometric is improved as compared to individual finger knuckle and finger vein. The fusion of these two modalities using Bayesian method demonstrated the recognition accuracy of 98.3%. Various weights of finger knuckle and finger vein affects the recognition accuracy. The better recognition accuracy is obtained at weight of finger knuckle is 0.8 and finger vein is 0.2. The performance index is improved i.e. 98.5% and the Error Equal Rate is 1.5%. The multimodal biometric recognition accuracy improved by these two fusion methods. Error equal rate is reduced by 10% than individual biometric system. The weighted sum fusion reduces error equal rate by 0.2 % as compared to Bayesian method. However multimodal system has the limitations of high setup cost, high computational complexity and non-standard classification rule. In the proposed algorithm, matching complexity is O [N (N-1) x M_1] for each biometric. Using conventional matching the complexity is O [N (N-1) x M_1 M_2]. For multimodal biometric using FK and FV, matching complexity is O 2[N(N-1) x M_1]. It shows great reduction in matching complexity using the proposed algorithms.

REFERENCES

[1]   Cheng-BoYu, Quin, LianZhang, Yan-Zhe Cui ,"Finger vein Image Recognition Combining Modified Hausdorff distance with minutia feature matching", Biomedical Science and Engineering. 2009

[2]   Naoto Miura, Akio Nagasaka, Takafumi Miyatake, "Extraction of Finger-Vein Patterns Using Maximum Curvature Points in Image Profiles", IAPR   Conference on Machine Vision Applications, Tsukuba Science City, Japan. 2005,

[3]   *Arun Ross, Anil k. Jain, "Multimodal Biometrics: An Overview", Proc. Of 12th European Signal Processing Conference (EUSIPCO), (Vienna Austria), September 2004, pp. 1221-1224.*

[4]   *[20] L.Hong, A.K. Jain, and S. Pankanti, "Can Multibiometrics improves performance?" in Proc. AutoID'99, Summit, NJ, USA. pp. 59 - 64.*

[5]   Zhang, Lei Zhang, David Zhang and Hailong Zhu, "Online Finger-Knuckle-Print Verification for Personal Authentication", Biometrics Research Center, Department of computing, The Hong Kong Polytechnic University

[6]   M. Indovina, U. Uludag, R. Snelick, A. Mink, A. Jain, "Multimodal Biometric Authentication Methods: A COTS Approach", National Institute of Standards and Technology, Michigan State University, Appeared in Workshop on MMUA, December 2003.

[7]   Ajay Kumar, Ch. Ravikanth , "Personal Authentication using Finger Knuckle Surface", IEEE Transactions on Information Forensics and Security, vol. 4, no. 1, March. 2009, pp. 98-110,

[8]   Lin Zhang, Lei Zhang, David Zhang, Zhenhua Guo, "Phase Congruency induced Local features for F i nger-knuckle-print R e cognition", Patten Recognition,45, 2012, pp. 2522-2531.

[9]   Michael K.O. Goh, Connie Tee, Andrew B.J. Teoh "BI-modal Palm Print And Knuckle Print Recognition System", Journal of IT in Asia, vol 3, (2010). (FKP4)

[10]   Shrotri A., Rethrekar S.C., Patil, M.H. Debnath, Bhattacharyya, Tai-hoonKim, "Infrared Imaging of Hand Vein Pattern for Biometric Purpose", Journal of Security Engineering2009.

[11]   Naoto Miura, Akio Nagasakat, Takafumi Miyataket, "Automatic Feature Extraction from non-uniform Finger Vein Image and its Application to Personal Identification", IAPR Workshop on Machine Vision Applications, Japan, 2002 .

[12]   Dana Hejitmankova, Radim Dvorak, Martin Drahansky, and Filip Orsag, "A new method of Finger Vein Detection", International journal of Bio-science and Biotechnology, **1**(1) , 2009

[13]   Laxmi C., Deepaka , Kandaswamy A., , "An Algorithm For Improved Accuracy in   Unimodal Biometric Systems through Fusion of Multiple Features Sets" ,ICGST-GVIP **9**(III), 2009

[14]   Jing Zhang, Jinfeng Yang, , " Finger-Vein Image enhancement Based on Combination of Gray-Level Grouping and Circular Gabor Filter ", IEEE,2009

[15]   Etta D., Pisano , Shuquan Zoog, Bradley m. Hemminger, Marla DeLuca, R . Eugene   Johnston, Keith Muller M. Patricia Braeuning, and Stephen Pizer, "Contrast Limited Adaptive Histogram Equilization Image processing to improve the Detection of Simulated Speculation in dense Mammograms", Journal of Digital Imaging, **11** (4) , 1998

[16]   Stephin M. Pizer,E. Philip Amburn, John D. Austin,Robert Cromartie, Ari Geselowtiz, Trey Greer,Bart Ter Haar Romeny, John B. Zimmerman, and Karel Zuiderveld, "Adaptive histogram Equalization and its Variations", Computer Vision, Graphics, and Image Processing, 39,355-368, ,

[17]   Tomasi C., Manduch R., "Bilateral Filtering for Gray and Color Images", in Proceedings of IEEE International Conference on Computer Vision, Bombay, India, 1998, pp 237-240

[18] H.B.Kekre and V.A.Bharadi, "Finger Knuckle Verification   using Kekre's Wavelet Transforms", International Conference & Workshop on Emerging Trends in   Technology, ACM Digital Library, New York; 2011. pp 32-37,

[19] H. B. Kekre, Archana Athawale, Dipali Sadavarti, "Algorithm to Generate Wavelet Transform from an Orthogonal Transform", International *Journal of Image Processing;* 2011.

[20] Sujata Kulkarni, Ranjana Raut and Pravin Dakhole, "Wavelet Based Modern Finger Knuckle Authentication", Accepted for publication Published by Elsevier B.V in proceedings 4th International Conference on Eco-friendly Computing and Communication Systems, NIT Kurusetra, India, Elsevier Publications Science Direct Procedia Computer science.

[21] Sujata Kulkarni, Ranjana Raut and Pravin Dakhole , "A Novel Authentication System Based on Hidden Biometric Trait" Accepted for publication in proceedings of   International Conference on Computational Modeling and Security (CMS 2016), Banglore, **Elsevier Publications** , Science Direct Procedia Computer science.

[22] Feifei CUI and Gongping Yang, "Score Level Fusion of Fingerprint and Finger Vein Recognition", Journal of Computational Information Systems 7: 16 (2011) 5723-5731

Automatic Segmentation and Classification of Masses from Digital Mammograms

[1]Basma A. Mohamed, [1]Nancy M. Salem, [1]Marwa M. Hadhoud and [1,2]Ahmed F. Seddik
[1]*Faculty of Engineering, Biomedical Engineering Department, Helwan University, Cairo, Egypt;*
[2]*Faculty of Computer Science, Nahda University (NUB) Egypt*
eng_basma1990@yahoo.com; nancy_salem@h-eng.helwan.edu.eg;
marwa_hadhoud@h-eng.helwan.edu.eg; ahmed_sadik@h-eng.helwan.edu.eg

ABSTRACT

Breast cancer is one of the leading causes of death among female cancer patients. Mammography is the most efficient method for the early detection of abnormalities that are associated with breast cancer. Masses and micro calcifications are the most popular abnormalities that indicate breast cancer. The proposed paper intends to develop an automated system for assisting the analysis of digital mammograms. First, a preprocessing step is applied to enhance images followed by a segmentation step that is based on morphological operations and Otsu's thresholding techniques. Thereafter, shape features are extracted from the segmented region and used in the classification process. Finally, the classification step to classify the segmented shape as round, oval, lobular, or irregular. The algorithm is tested using 270 mammogram images from the Women Health Care Program (WHC) and 142 publicly available images from the Digital Database for Screening Mammography (DDSM). Results show that the proposed technique effectively detects and segments masses from mammogram images. The shape of segmented masses is classified into either round, oval, lobular, or irregular. Round and oval shapes are classified with 100% accuracy while lobular and irregular shapes results in accuracy of 93% using the ANN for the WHC dataset and 100%. On the other hand, accuracy for images from the DDSM is 100% and 91.3% respectively.

Keywords: Breast Cancer, Digital Mammograms, Otsu's threshold, BI-RADS™ Categories.

1   Introduction

Breast cancer is the most commonly detected type of cancer among women all over the world. Due to the unawareness, there is an increase in the cases that are detected and diagnosed in advanced stages of the cancer [1]. To help in the early detection of this type of cancer, screening programs are required to detect the early signs of the breast cancer. Currently, mammography is a very effective method for the early detection of masses or abnormalities. It can detect 85 to 90 percent of all breast cancers. Masses and micro calcifications are signs that indicate breast cancer.

According to Breast Imaging Reporting and Data System (BIRADS), the shape, size, margins, and density are the features that are used to characterize masses [2-4]. The shape could be round, oval, lobular, or irregular. The shape and margin properties play an important role in classifying the masses. It is observed that benign tumors have a round, oval or lobular shapes while malignant have irregular or lobular shapes with a speculated margin. With the advances in computer technology, Computer-aided detection systems (CAD) have been developed to improve breast cancer screening and

diagnosis. The CAD system helps in processing large number of images and it involves digital image processing, image analysis, artificial intelligence, and software development.

In the literature, many methods have been developed for the detection and classification of masses or microcalcifications [5-13]. For the detection of masses, the Growing Neural Gas (GNG) has been used with the Supported Vector Machine (SVM) [5]. A sensitivity of 89.3% is reported when using a set of 997 images from the DDSM database. In the work proposed by Tzikopoulosa et al. [6], the breast density estimation and the asymmetry detection are used for the segmentation and classification of mammograms from the mini-MIAS database. Statistical features for pair of mammograms were computed and the difference is used to define the asymmetry followed by SVM with a success rate of 84.47%.

Region growing and Wavelet Transform are used in the work proposed in [7]. Features are extracted and the classification is performed using the SVM. Images were used from the MIAS database and a local dataset from the hospital of Istanbul University (I.U.) in Turkey. The K-means clustering method is used in [8] to detect masses. A set of 650 images from the DDSM database is used and results in a sensitivity of 83.24%, and a specificity of 84.14%. The Artificial Neural Network (ANN) is used with shape and texture features in [9]. A set of 226 images (109 malignant and 117 benign masses) were used. The sensitivity and specificity are 78.1% and 79.1% respectively.

Regarding the shape of the masses, Vadivel and Surendiran [10, 11] developed an algorithm for classifying masses into the four basic shapes; round, oval, lobular, and irregular. Shape features have been extracted and then the feature vector is applied to the C5.0 decision tree algorithm and fuzzy inference systems. The algorithm is tested using 224 mammogram masses from DDSM database. They achieved accuracy of 87.76% in differentiating the four mass shapes, 100% in differentiating between round and oval masses, and accuracy 93.29% in differentiating between lobular and irregular masses [11].

The SVM and the Linear Discriminant Analysis (LDA) have been used to classify 200 and 3600 regions of interest from the MIAS and DDSM databases respectively. Results from the two classifiers are compared and results show a better performance for the SVM as reported by Costa et al. [12].

In this paper, a new method to segment and classify masses from digital mammograms is proposed. This paper is organized as follows: Section 2 presents the proposed detection and classification method. Section 3 describes the experimental results and the conclusion is given in Section 4.

2 Proposed Method

This section describes the proposed method for detection and classification of mases from digital mammograms. Figure 1 shows a block diagram of the proposed method and its four main stages. In the beginning, a preprocessing is applied to enhance images followed by a segmentation stage that is based on morphological operations and Otsu's thresholding techniques to detect masses. Thereafter, shape and texture features are extracted from the segmented region. Finally, the classification stage which consists of two sequential steps; the first one to distinguish masses as either regular or irregular. The second step is applied to distinguish the regular mass as either oval or round and the irregular mass as either lobular or irregular. Three different classifiers have been used in the classification stage which are: the ANN, the SVM and the K-Nearest Neighbor classifier (KNN).
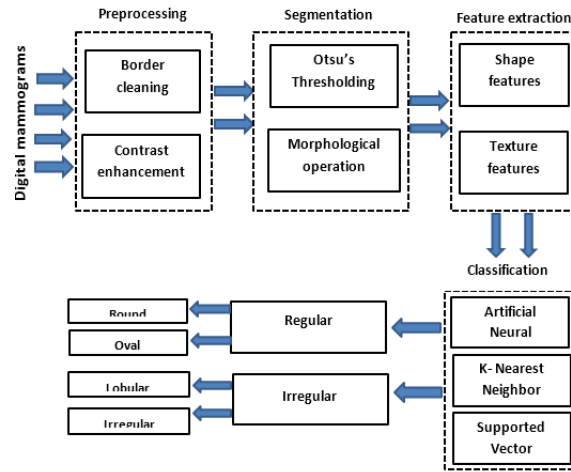
Figure 1: Block diagram of the proposed method.

2.1 Datasets

In this study, two different databases are used. 270 images have been collected from Women Health Care Program (WHC) [14], which is a large-scale initiative for women's healthcare comprising digital mammograms for early detection of breast cancer. These images were previously investigated and labelled by expert radiologists based on technical experience and biopsy. The database contains 270 mammograms including 185 malignant and 85 benign cases (73 are round, 83 are oval, 18 are lobular and 96 are irregular). All images are digitized at a resolution of 2294x1914 pixels. 142 mammograms have also been used from the DDSM digital image database [15] that contains 96 malignant and 46 benign masses (7 are round, 17 are oval, 21 are lobular and 96 are irregular).

2.2 Pre-processing

A pre-processing stage is required to improve the image quality and to enhance the segmentation results. Image border cleaning is applied to remove any artifacts like the pectoral muscle and any labels attached to the border of the image. Then the intensity adjustment is applied to improve the contrast between the mass structures and surrounding texture of the breast tissues. These steps are shown in Figure 2.
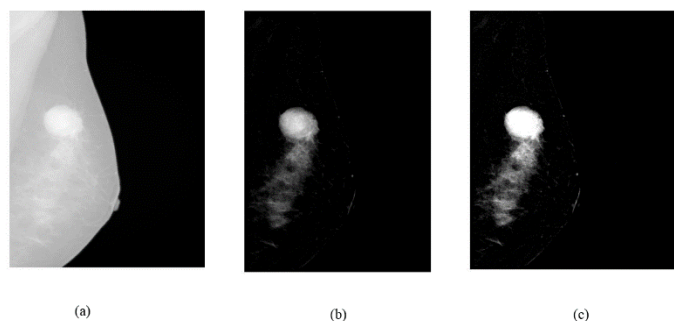

Figure 2: The preprocessing stage: (a) Original mammogram, (b) Border clearing, and (c) Contrast adjustment.

2.3 Mass Segmentation

The goal of segmentation stage is to identify the region of interest (mass) and this is achieved by applying the Otsu's threshold [16] and morphological operations [17] such as erosion and opening to extract this region. In this paper, the Otsu's threshold technique alone is not efficient enough to get a good result in identifying the mass region, so a constant is added to a global threshold that can be

used to convert an intensity image to a binary image. The constant value lies between 0 and 1. Figure 3 shows segmented masses.
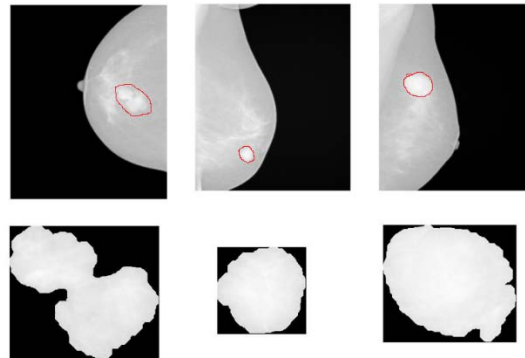
Figure 3: Examples of extracted masses.

2.4 Feature Extraction

Feature extraction is very important in the classification of masses. There are many different features that are used in mass classification; the most common features are texture and shape features. The BIRADS specifies that benign masses are round, oval, lobular and malignant masses are lobular or irregular shape. In this work, shape and texture features such as area, perimeter, major axis, minor axis, thinness ration, eccentricity, equivdiameter, dispersion, compactness, circularity, roundness, elongation, shape index and entropy. These features are extracted from segmented regions and then the features are normalized and ranked using absolute value two-sample t-test to select the most effective features.

2.5 Classification

In this stage, the segmented mass is firstly classified as either regular or irregular; then the regular masses are classified into round or oval and the irregular masses into lobular or irregular. In this paper, a comparison is performed between ANN [18], K-Nearest Neighbor [19] and SVM.

3 Experiments and Results

The MATLAB 2015 software is used to implement the proposed algorithm. In the beginning, the pectoral muscle removal and image enhancement were applied to improve the mass segmentation. As mammograms have different intensity contrast levels as a result of various breast density levels for different patients, it is difficult to select an optimal image enhancement technique. Masses were brighter than the surrounding area, so it can be detected and segmented by thresholding. The Otsu threshold is used to obtain a binary image followed by morphological operators to remove isolated pixels that are not related to the mass. Experiments show that results of the mass detection improved when adding a predefined constant the threshold value obtained by the Otsu threshold algorithm.

For images from the WHC, the segmentation results in masses detection with 100% accuracy. For images from the DDSM, accuracy of 90% is obtained.

Segmented masses are used to extract 15 shape and margin features. These features are extracted from segmented regions and then features are normalized and ranked using absolute value two-sample t-test to know the most significant features. The features are ranked as follows:

Thinness ratio	Major axes /minor axes
Compactness	Perimeter
Elongation	Area/perimeter
Shape index	Major axes
Circularity 1	Dispersion
Entropy	Equiv diameter
Eccentricity	Area
	Minor axes

The classification stage consists of two steps; first step is to classify masses as either regular or irregular. Experimental results for classifying the masses as either regular or irregular of the first and second databases are shown in Figure 4. Different numbers of features have been used with three different classifiers. As shown in Figure 4-a for the WHC dataset, when using the thinness ratio only, a result of 100% is obtained with the three classifiers. Best results obtained when using the ANN with less number of features and then decreased with increasing the number of features. Second best results obtained when using the SVM classifier. The KNN has better performance with two to four features only.

As shown in Figure 4-b for mammograms from the DDSM dataset, best results obtained when using a feature vector of seven to 11 feature with the ANN or the SVM. Results using the KNN is about 93%.
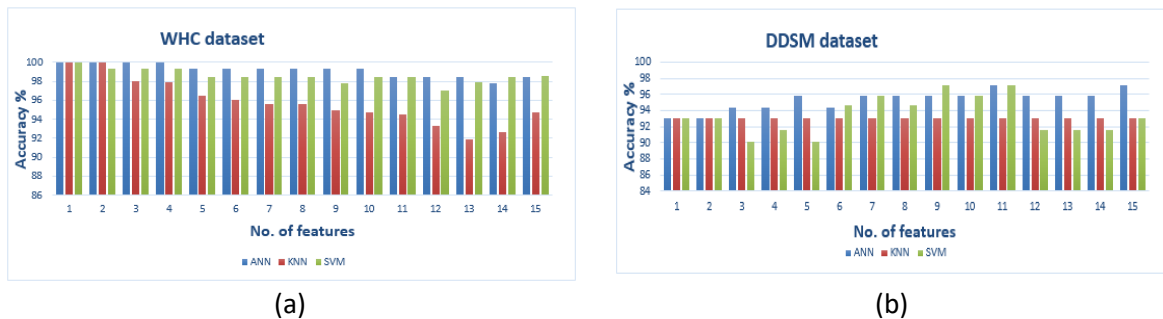

(a)   (b)

Figure 4: First classification step using: (a) WHC dataset, and (b) DDSM dataset

The second step of the classification is used to classify regular masses into round or oval and irregular masses into lobular or irregular. Results of this step are summarized in Table 1 when one feature (roundness) only is used. A comparison between the proposed method and other methods from the literature is summarized in Table 2.

Results are compared to these reported in [10, 11]. The proposed algorithm used less number of features for the first classification step. It is important to declare that a very good performance is obtained when using thickness ratio as one feature in the first step with the ANN, SVM and KNN with the WHC dataset. A set of seven to eleven features were enough to get good performance with the DDSM dataset. On the other hand, there is only one feature is used in the second step of classification

Table 1: Performance of the second classification step.

Dataset	Shape	Accuracy %		
		ANN	KNN	SVM
WHC dataset	Round vs. oval	100 %	100 %	98.7 %
	Lobular vs. irregular	93 %	92 %	84 %
DDSM dataset	Round vs. oval	100 %	100 %	92.9 %
	Lobular vs. irregular	91.3 %	90 %	85 %

Table 2: Performance comparison

Methods	Database	No. of Features	Classifier	Accuracy	
				RO	IL
Surendiran [10]	DDSM	19	ANN	98.32 %	NA
Vadivel [11]	DDSM	17	Fuzzy inference system	100 %	93.29 %
Proposed method	WHC Local dataset	15	ANN	100 %	93 %
			KNN	100 %	92 %
			SVM	98.7 %	84 %
	DDSM	15	ANN	100 %	91.3 %
			KNN	100 %	90 %
			SVM	92.9 %	85 %
Where I = Irregular, L= Lobular , R= Round and O = Oval					

4 Conclusion

In this paper, an algorithm for automated detection and classification of masses in digital mammograms is proposed. The method consists of four main stages, preprocessing, segmentation, feature extraction, and classification. The proposed algorithm is tested using a set of 270 digital mammogram images from the WHC and 142 mammograms from the DDSM digital image database. Results show that the proposed technique effectively detects and segments all masses from the mammogram images with accuracy of 100 % and 90% for the WHC and DDSM datasets respectively. The classification stage consists of two steps. Comparable results were obtained when using the ANN classifier to other methods in the literature. In this paper, three different classifiers were tested and results show a good performance for the ANN compared to the KNN and SVM.

REFERENCES

[1] Breast Cancer Foundation of Egypt (BCFE), http://www.bcfe.org/en/index.php, 2014.

[2] Verma, B., P. McLeod, and A. Klevansky, A novel soft cluster neural network for the classification of suspicious areas in digital mammograms, Pattern Recognition, 2009. 42 (9): p. 1845-1852.

[3] Heath, M., et al., The digital database for screening mammography, Proceedings of the International Workshop on Digital Mammography 2000. p. 212-218.

[4] ACR, Breast imaging reporting and data system (BI-RADS), Breast Imaging Atlas, 4th ed., American College of Radiology, Reston, VA, 2010.

[5] Oliveira Martins, L., et al., Detection of breast masses in mammogram images using growing neural gas algorithm and Ripley's K function, Journal of Signal Processing Systems, 2009. 55 (1 –3): p. 77-90.

[6]   Tzikopoulosa, S., et al., A fully automated scheme for mammographic segmentation and classification based on breast density and asymmetry, Computers Methods and Programs in Biomedicine, 2011. (102): p. 47-63.

[7]   Görgel, P., A. Sertbas, and O. Ucan, Mammographical mass detection, and classification using Local Seed Region Growing– Spherical Wavelet Transform (L SRG– SWT) hybrid scheme, Computers in Biology and Medicine, 2013. 43: p. 765-774.

[8]   Nunes, A., A. Silva, and A. Paiva, Detection of masses in mammographic images using geometry, Simpson's Diversity Index and SVM, Journal of Signal and Imaging Systems Engineering, 2010. 3(1): p. 43-51.

[9]   Retico, A., et al., An automatic system to discriminate malignant from benign massive lesions on mammograms, Nuclear Instrumentation and Methods in Physics Research, 2006. 569(2): p. 596-600.

[10]   B. Surendiran and A. Vadivel, Classifying mammographic masses into BI-RADSTM shape categories using various geometric and shape features, International Journal of Biomedical Signal Processing, 2011. 2(1): p. 43-47.

[11]   Vadivel, A., and B. Surendiran, A fuzzy rule-based approach for characterization of mammogram masses into BI-RADS shape categories, Computers in Biology and Medicine, 2013. 43: p. 259-267.

[12]   Costa, D., et al., Independent component analysis in breast tissues mammograms images classification using LDA and SVM, Information technology Application in Biomedicine, 2007. p. 231-234.

[13]   De Nazar Silva, J., et al., Automatic detection of masses in mammograms using quality threshold clustering, correlogram function, and SVM, Journal of Digital Imaging, 2015. 28 (3): p. 323-373.

[14]   Women Health Care Program, http://www.whop.gov.eg, 2007.

[15]   Heath, M., K. Bowyer, and D. Kopans, Current status of the digital database for screening mammography, Digital Mammography, Kluwer Academic Publishers: p. 457-460.

[16]   Otsu, N., A threshold selection method from gray-level histograms, Systems, Man, and Cybernetics, IEEE Transactions on, 1979. 9(1): p. 62-66.

[17]   Gonzalez, R., R. Woods, and S. Eddins, Digital image processing using MATLAB, Gatesmark Publishing; 2nd edition, 2009.

[18]   Schalkoff, R., Artificial neural networks. McGraw Hill, Publishers, 1997. p. 146-118.

[19]   Altman, N. S., An introduction to kernel and nearest-neighbor nonparametric regression. The American Statistician, 1992. 46(3): p. 175-185.

Technology-Assisted Carpal Tunnel Syndrome Rehabilitation using Serious Games: The Roller Ball Example

Loannis Pachoulakis and Diana Tsilidi

Department of Informatics Engineering, Technological Educational Institute of Crete, Heraklion-Crete, Greece;
ip@ie.teicrete.gr; dtsilidi@gmail.com

ABSTRACT

The adverse effects of improper posture and unhealthy computer usage habits on human physiology have been well documented. Prominent among these, the Carpal Tunnel Syndrome (CTS) is a medical condition where the median nerve passing through the wrist's carpal tunnel is compressed causing pain, numbness and tingling in affected parts of the hand. Depending on the severity of the symptoms, treatment may include physiotherapy and/or surgery. The present paper discusses possibilities that technology-driven physiotherapy based on serious games can augment a more traditional physiotherapy exercise curriculum. Accordingly, we present a Unity3D game called Roller Ball, the scenario of which combines CTS-specific physiotherapy exercises in a natural scenario-based way to guide a ball across a bridge in a 3D scene. The game employs the Leap Motion sensor, whose detailed wrist and hand (including fingers) tracking abilities make it a promising hardware platform for rehabilitation oriented exercises intended for patients suffering from CTS.

Keywords: Carpal Tunnel Syndrome, Physical Therapy, Leap Motion, Sensors, Serious Games.

1   Introduction

Carpal tunnel syndrome (CTS) is a medical condition in which the median nerve is compressed as it travels through the wrist's carpal tunnel, causing pain, numbness and tingling in parts of the hand that receive sensation from the median nerve [1]. Many patients resort to physiotherapy to reduce the pain and follow an exercise schedule for mobility and strength. Conservative management of symptoms related to CTS include exercises which involve tendon gliding of the finger flexor tendons and nerve gliding of the median nerve [2], [3]. Individualized therapy may also include additional exercises to increase muscle strength in the hand, fingers and forearm – and in some cases, the trunk and postural back muscles – as well as stretching exercises to improve flexibility in the wrist, hand and fingers. The goal of physical therapy is to reduce the severity of symptoms, to possibly eliminate the need for surgery and to permit the patient to be active and functional in everyday life. Physical therapy is also important following CTS surgery to help patients restore strength to the wrist and to retrain them to stray from the bad habits that may have led to the symptoms in the first place [4]. However, physical therapy is a slow process and it often takes weeks or months before positive effects are felt. During therapy, patients have to perform time consuming, repetitive and, as a result, boring exercises. Whereas in some cases the presence of a physical therapist may not be strictly necessary after the first few establishing sessions, in other cases mounting physiotherapy expenses may make it difficult to schedule sessions as frequently as may be required. It is fairly common for patients to attend a number of intensive physiotherapy sessions and then be given an exercise curriculum and schedule to

follow at home on a regular basis, checking with the physiotherapist more sparingly. As lack of motivation arising from the repeatability and predictability of the exercises sets in, patients begin to neglect to perform their exercise program at home as regularly as they should [5]. Therefore, transforming traditional physiotherapy exercises into interesting and hopefully fun games carries a special promise to unsupervised therapy, as goal oriented, highly interactive games can provide the necessary motivation to carry out and complete an exercise schedule at home. In addition, game features such as being in control of a 3D world, combined with elements such as achievements, high scores, rewards and positive feedback, can draw patients to lengthier game sessions and thus speed up their recovery [6].

The effectiveness of a therapeutic game system is commonly based on assessing patient progress during rehabilitation. Sensor technology has matured sufficiently to persuasively and un-obstructively be integrated in game solutions. Indeed, three ubiquitous motion tracking sensors in today's games (Nintendo's Wii, Microsoft's Kinect and the Leap Motion sensor) have different philosophies and follow different approaches to bring motion capture to their host game platforms. Nintendo's Wii, released in 2006, was the first home video game console to use motion-sensing technology [7]. The primary Wii remote controller detects movement in three dimensions. In addition to the usual buttons, it has a built-in accelerometer combined with infrared camera which allows it to sense its position in 3D space and detect acceleration along three axes. The remote controller connects to Wii using Bluetooth with an approximate range of 9 meters. Additional Wii-compatible controllers include the Nunchuck (which features an accelerometer and a traditional analog stick with trigger buttons) as well as a Balance Board which contains several sensors that calculate the mass of the player standing on it and his/her center of gravity. There have been attempts to combine the benefits of Nintendo's Wii with other projects to produce new integrated rehabilitation systems [8].

Wii has a large user base and has been effective in exercising the entire human body. For example, post-stroke patient condition has shown to improve after the use of Wii Fit Balance Board for rehabilitation. Whereas many Wii-based games make use of the Balance Board extension, it is a risky piece of hardware for Parkinson's disease patients, as it may lead to falls [9]. In addition, all Wii games require a handheld controller to capture the player's movement, which may be troublesome for some patients. In addition, excessive game play, tiredness and the enthusiasm of group play may lead to injuries related to falls or player body part collisions. Cases reported include acute tendonitis of right infraspinatus, dislocation of left patella, medial meniscal tear, and acute onset of carpel tunnel syndrome (see for example [10], also [11]). Finally, Wii's remote control is supposed to be grasped and does not allow delicate hand movements (flexions, extensions, deviations).

Microsoft's Kinect is a motion sensor bar initially built as an alternative input device to a remote control to the Xbox 360 video game console and later also released for Windows PCs. Kinect uses a Natural User Interface (NUI) to enable user interaction with the game environment through gestures or voice commands. The sensor bar contains an RGB camera and a depth sensor composed of an infrared emitter and a monochrome CMOS to offer robust 3D data capturing as well as a multi-array microphone used to isolate players' voices from the noise in the room. The supporting Software Development Kit (SDK) enables recognition of six players and can provide continuous skeletal tracking of two of them and can be programmed in C++, C#, and Visual Basic.Net [12].

Evaluation of the Kinect sensor in medical applications requiring a motion capture device show that it is capable of sufficiently precise skeleton joint tracking in many physical therapy and rehabilitation treatments requiring large "macroscopic" movements of body parts. At the same time, there are some skeleton tracking issues arising from data noise and false recognition of some scene objects. As an

example, confusing a chair's leg with a siting patient's leg incapacitates the development of applications for individuals using wheelchairs or walkers. The results of clinical experiments with volunteers asked to perform arm and leg abductions and flexions showed that Kinect tracks movement accurately but it may underestimate arm movements and overestimate leg movements by up to 30% [13].

Techniques such as computational algorithms are also used to reduce tracking errors and improve Kinect's motion tracking accuracy. However, due to the appreciable random positional errors involved, the Kinect sensor is an appropriate therapeutic tool for wrist/hand joint tracking.
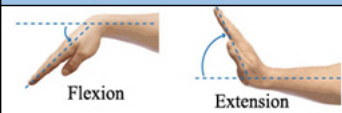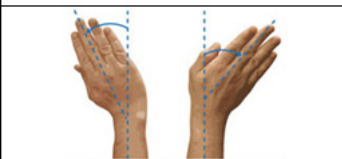
At present, the most promising candidate sensor for technology-based CTS-oriented rehabilitation seems to be the Leap Motion controller, a small USB peripheral device which is commonly placed on a table, facing upward. Using two monochromatic IR cameras and three infrared LEDs, the device commands a roughly hemispherical area out to a distance of about 1 meter from the sensor. The LEDs generate pattern-less IR light and the cameras generate frames of reflected data at a rate of close to 300 fps. This data stream is fed to the host computer through a USB cable, where Leap Motion's supporting software combines concurrent 2D frames generated by the two IR cameras to generate accurate synthetic 3D position data for the hand
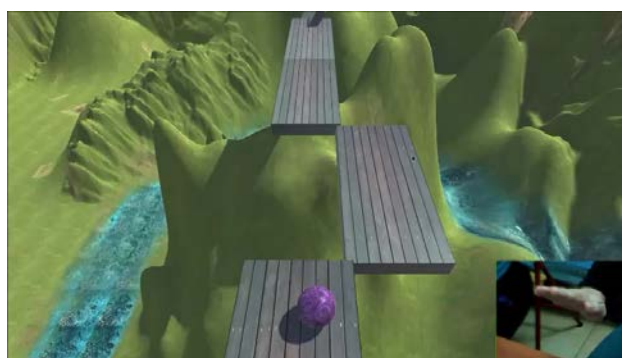
Figure 1: Sample screen-shot from the Roller Ball game tailored to Carpal Tunneling Syndrome rehabilitation. Using CTS specific exercises such as extension/flexion and radial/ulnar deviation, the patient has to successfully guide a ball on a continuously reconfigurable bridge, while avoiding a number of moving obstacles. The insert in the bottom right part of the screen-shot shows the wrist currently in an extension gesture to hold the ball back from moving ahead.

In a study conducted by [14], the Leap Motion sensor was employed in an open source (JavaScript) version of the game Fruit Ninja for stroke patient rehabilitation. The original game was modified for the needs of the study and mouse events were replaced by hand movement tracking. The pilot study involved 14 patients with stroke, who were asked to play the game for one minute, while they were able to choose the appropriate difficulty level for their condition. The results showed a general satisfaction of the users, who considered this way of rehabilitation engaging, useful and would use it at home. In this work we explore key advantages and capabilities of the Leap Motion sensor for the creation of CTS-oriented serious games. Accordingly, we have created a 3D serious game called Roller Ball – a relevant screen-shot of which appears in Figure 1 – which requires users to perform CTS-specific exercises (extensions/flexions and radial/ulnar deviations of the wrist, shown in Figure 2) to successfully guide a ball over a continuously reconfigurable bridge without falling in the void below. The bridge is made of planks, some of which periodically move to form gaps and discontinuities. In

addition, a number of moving obstacles must be avoided to make it to the other end of the bridge without being knocked out of it.


Figure 2: The left column presents four wrist physiotherapy exercises commonly used to treat Carpal Tunnel Syndrome. Each exercise is detected in the game as a gesture and is mapped onto an action on the ball as shown in the right column.

2 Roller Ball: A Serious Game tailored to Carpal Tunnel Syndrome based on the Leap Motion Sensor

The Roller Ball game is developed in Unity3D and uses CTS-specific physiotherapy exercises to guide a ball across a 3D scene along a bridge, while trying to avoid moving obstacles or fall off the bridge. Relevant game scenes appear in Figures 1, 3 and 4. The CTS-specific exercises used to guide of the ball appear in Figure 2 and include Flexion/Extension for the Go/Stop ball movement and Radial/Ulnar deviation to move the ball to the left/right, respectively (depending on which hand is being exercised). To make the game more challenging to the user, if one of the above gestures is not detected, the ball moves forward along a straight path at a low constant speed. Leap Motion's supporting software combines concurrent 2D frames generated by two IR cameras to generate accurate synthetic 3D position data for the hand. For each such frame, the Leap Motion API (discussed for example in [15]) uses the frame () method to expose captured motion tracking data to the application developer. This data is organized in the form of physical entities: hands, fingers and tools. A frame buffer maintains the most recent 60 frames so that a "history" parameter to the frame () method can be used to retrieve a required number frames starting from the current frame. In addition, the Frame class defines several functions that extracts useful frame data, such as a hand's position, orientation, posture, and motion:

- isRight, isLeft – parameters that identify the hand being tracked.
- Palm Position – the distance from the center of the palm to the origin of the sensor in millimeters.
- Palm Velocity – the speed and direction of movement of the palm in millimeters per second.
- Palm Normal – a vector perpendicular to the plane formed by the palm of the hand pointing downward and out of the palm.
- Direction – a vector pointing from the center of the palm toward the fingers.
- grabStrength, pinchStrength – parameters that describe the posture of the hand.
- Motion factors – a parameter group that provides relative scale, rotation, and translation factors for movement between two frames.

Finally, the Vector class defines functions for getting the pitch (angle around the x-axis), yaw (angle around the y-axis), and roll (angle around the z-axis).
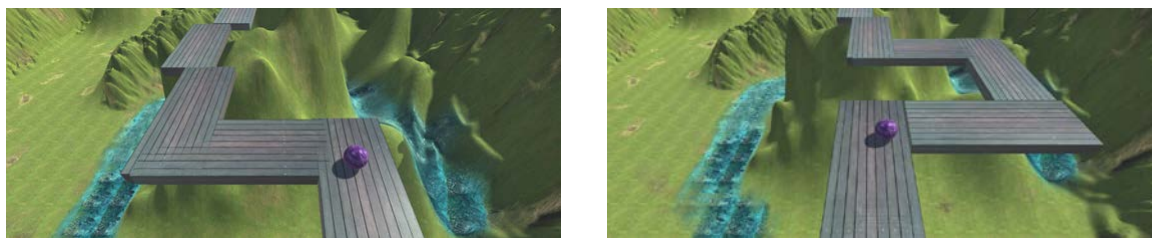
Figure 3: The top figure (a) is a screen capture showing a game scene that requires turning the ball to the left. This can be accomplished either by radial deviation of the right hand or an ulnar deviation of the left hand, depending on which hand is being exercised. Similarly, to turn the ball to the right as is required in the game scene shown in the bottom figure (b), the player must employ either an ulnar deviation of the right hand or a radial deviation of the left hand

Some customization in the response of the game to patient input is dictated by the fact that, even for a healthy hand and wrist, the angular extent for radial deviation is more limited than that for an ulnar deviation (Figure 2Figure 1). This affected the set of parameter values responsible for successful gesture detection (radial versus ulnar deviation). Further customization is naturally possible on a perpatient basis depending on the severity of the symptoms to permit exercising to the fullest range of motion that is possible to a particular patient.
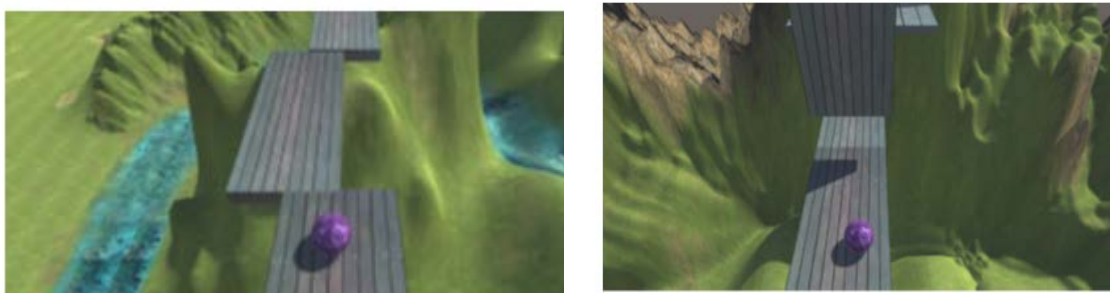
Figure 4: An obstacle in the game scene that requires wrist flexion or extension (flexion will move the ball forward, while extension will stop the ball's movement)

The game scene and the obstacles were designed to serve a game scenario that demands repetitive player actions, since in traditional physiotherapy the patient has to repeat certain movements at a specific pace. Figure 3 relates two sample game scenes. The game scene shown in Figure 3(a) requires that the player guides the ball to a left turn through either an ulnar deviation of the left hand or via a radial deviation of the right hand. By comparison, the game scene in Figure 3(b) requires that the player guides the ball to a right turn through either a radial deviation of the left hand or via an ulnar deviation of the right hand. Extension stops the movement of the ball, while flexion moves the ball forward. These wrist-hand postures can be used in game contexts such as those displayed in Figure 4. At this point it should be mentioned that the patient should use one hand for a given session so that both hands can perform the prescribed exercises correctly.

The obstacles situated in the game scene add to a more interesting and at the same time challenging game environment. Obstacles can be avoided and challenges can be surpassed by carefully timing and maintaining wrist-hand postures such as wrist flexion/extension and/or radial/ulnar deviation. At the

same time, these obstacles urge patients to use flexion and extension of the wrist, i.e. rotation of the wrist downwards and upwards. For example, Figure 4(a) shows a board further down the bridge that constantly moves from right to left and back so that the patient must time the movement of the ball in a way that it passes over that moving plank quickly while it connects to the previous and next planks.

Another challenge appears in Figure 4(b), where a swinging vertical plank may knock the ball off the bridge. To avoid this, the patient must combine flexion and extension to time a safe passage of the ball across the obstacle. In addition, whereas in some cases the player can freely choose the movement, in other cases and depending on the form and movement of the obstacle, the player has to use specific a hand movement to avoid the particular obstacle. For example, more challenging scenarios allow for a sloped bridge where the ball develops may pick up or lose speed due to gravity. In these cases the user will be forced to perform prescribed exercises to greater deviations in a natural scenario-dependent manner.

3 Discussion and Future Work

In this work we investigate the potential of the Leap Motion sensor as a hardware platform on which to base serious games for the rehabilitation of patients suffering from Carpal Tunnel Syndrome (CTS). Accordingly we have presented the Roller Ball game which has been developed Unity3D to explore the possibilities and limitations of the sensor and concluded that the tracking accuracy of the sensor is sufficient to detect and track certain wrist-hand postures required by physiotherapy exercises used to alleviate CTS symptoms. Limitations in the applicability of the sensor for the intended purpose arise naturally in CTS-specific exercises where the wrist-hand posture causes part of the hand (e.g., fingers) to be physically occulted by other parts. In some of these cases the obstacles can be alleviated by removing the sensor from the default location (table top) and attaching it to a fixture that allows its re-orientation so as to view the hand from another point of view (e.g., from the top or one side).

The use of Leap Motion sensor in physical therapy and rehabilitation may appear limited, because it appropriately tracks the lower arm, hand and fingers. However this is sufficient for serious games tailored to CTS patients. In addition, the sensor can be used in conjunction with other existing platforms to be allow the calculation of additional metrics and detect and track a richer set of gestures [5]. For example, the Leap Motion sensor can be paired with Microsoft's Kinect to provide the required precision in the detection of hand gestures like pronation/supination and flexion/extension of metacarpophalangeal and the proximal interphalangeal joints of the hand, while Kinect provides larger scale body tracking. Finally, technology-enabled rehabilitation can offer measurable results as games can be designed to collect performance data and use these to calculate and store appropriate performance metrics. This possibility should allow therapists to assess long term progress and to mitigate a sense of accomplishment to the patients which can be very beneficial during treatment [16].

REFERENCES

[1]   R. A. Werner and M. Andary, "Carpal tunnel syndrome: pathophysiology and clinical neurophysiology," *Clin. Neurophysiol.*, vol. 113, no. 9, pp. 1373–1381, Sep. 2002.

[2]   S. L. Michlovitz, "Conservative interventions for carpal tunnel syndrome.," *J. Orthop. Sports Phys. Ther.*, vol. 34, no. 10, pp. 589–600, Oct. 2004.

[3]   L. M. Rozmaryn, S. Dovelle, E. R. Rothman, K. Gorman, K. M. Olvey, and J. J. Bartko, "Nerve and tendon gliding exercises and the conservative management of carpal tunnel syndrome," *J. Hand Ther.*, vol. 11, no. 3, pp. 171–179, Jul. 1998.

[4]   "Physical Therapist's Guide to Carpal Tunnel Syndrome." [Online]. Available: http://www.moveforwardpt.com/symptomsconditionsdetail.aspx?cid=9f3cdf74-3f6f-40ca-b641-d559302a08fc. [Accessed: 05-Mar-2016].

[5]   A. Rahman, "Multisensor Serious Game-Based Therapy Environment for Hemiplegic Patients," *Int. J. Distrib. Sens. Networks*, vol. 2015, 2015.

[6]   "Making Physical Therapy Fun with Ten Ton Raygun." [Online]. Available: http://blog.leapmotion.com/axlr8r-spotlight-making-physical-therapy-fun-with-ten-ton-raygun/. [Accessed: 05-Mar-2016].

[7]   J. C. Lee, "Hacking the Nintendo Wii Remote," *IEEE Pervasive Comput.*, vol. 7, no. 3, pp. 39–45, Jul. 2008.

[8]   F. Anderson, M. Annett, and W. F. Bischof, "Lean on Wii: Physical rehabilitation with virtua reality Wii peripherals," *Stud. Health Technol. Inform.*, vol. 154, pp. 229–234, 2010.

[9]   G. Barry, B. Galna, and L. Rochester, "The role of exergaming in Parkinson's disease rehabilitation: a systematic review of the evidence.," *J. Neuroeng. Rehabil.*, vol. 11, no. 1, p. 33, 2014.

[10]   D. Sparks, D. Chase, and L. Coughlin, "Wii have a problem: a review of self-reported Wii relate injuries," *Inform. Prim. Care*, vol. 17, no. 1, pp. 55–7, 2009.

[11]   M. J. D. Taylor, D. McCormick, T. Shawis, R. Impson, and M. Griffin, "Activity-promoting gaming systems in exercise and rehabilitation," *J. Rehabil. Res. Dev.*, vol. 48, no. 10, p. 1171, 2011.

[12]   H. Mousavi Hondori and M. Khademi, "A Review on Technical and Clinical Impact of Microsoft Kinect on Physical Therapy and Rehabilitation," *J. Med. Eng.*, vol. 2014, pp. 1–16, 2014.

[13]   S. Obdrzalek, G. Kurillo, F. Ofli, R. Bajcsy, E. Seto, H. Jimison, and M. Pavel, "Accuracy and robustness of Kinect pose estimation in the context of coaching of elderly population," in *2012 Annual International Conference of the IEEE Engineering in Medicine and Biology Society*, 2012, pp. 1188–1193.

[14]   M. Khademi, H. Mousavi Hondori, A. McKenzie, L. Dodakian, C. V. Lopes, and S. C. Cramer, "Free-hand interaction with leap motion controller for stroke rehabilitation," in *Proceedings of the extended abstracts of the 32nd annual ACM conference on Human factors in computing systems - CHI EA '14*, 2014, pp. 1663–1668.

[15]   "Leap Motion API Reference." [Online]. Available: https://developer.leapmotion.com/documentation/csharp/api/Leap_Classes.html?proglang=csharp.[Accessed: 05-Mar-2016].

[16]   "What if Physical Rehabilitation Were as Easy as Playing a Video Game? - Not Impossible." [Online]. Available: http://www.notimpossiblenow.com/lives/what-if-physical-rehabilitation-were-as-easy-asplaying-a-video-game. [Accessed: 05-Mar-2016].